



Methyl Orange adsorption by reuse of a waste adsorbent poly (AAc/AM/SH)-MB superabsorbent hydrogel: matrix effects, adsorption thermodynamic and kinetics studies

Tripti Singh, Reena Singhal*

Department of Plastic Technology, Harcourt Butler Technological Institute, Kanpur 208002, UP, India
Tel. +91 512 2534001 05; Fax: +91 512 2533812; email: reena_singhal123@rediffmail.com

Received 31 May 2013; Accepted 8 October 2013

ABSTRACT

The traditional method for the treatment of used adsorbents is usually recovery for recycling or direct discarding them. In the present study, a more potential and economical method is described to reutilize a waste adsorbent. Poly(AAc/AM/SH) SAHs have proved to be a good adsorbent for cationic MB dye, and after adsorption, the SAHs were recovered for recycling. In this work, the waste MB dye loaded poly(AAc/AM/SH) SAHs were not recovered but directly applied to adsorb an anionic MO dye from another waste solution. The poly(AAc/AM/SH) SAHs after the MB dye adsorption were stable and suitable for MO dye adsorption for altered surface structures within a wide pH range. The various factors affecting the MO dye adsorption, including pH, contact time, ionic strength, initial concentration of the MO dye, and temperature, were systematically investigated. The equilibrium adsorption data fitted very well to the Langmuir adsorption isotherm and the maximum MO dye adsorption capacity reached to a high of 134 mg/g at 30°C. The thermodynamic parameters such as ΔH^0 , ΔG^0 , and ΔS^0 for the MO dye adsorption processes onto the SAHs were also evaluated, and the obtained negative ΔG^0 and ΔH^0 values confirmed that the MO adsorption process was spontaneous as well as exothermic. The kinetic studies indicate that the MO dye adsorption process was well consistent with the pseudo-second-order kinetic model. The desorption studies showed that the regeneration of the poly(AAc/AM/SH)-MB SAHs adsorbent can be easily achieved.

Keywords: Hydrogels; Sodium humate; Adsorption kinetics; Methyl Orange adsorption; Thermodynamic parameter

1. Introduction

Wastewaters from industries like dyeing, textile, printing, food coloring, cosmetics, and papermaking, are the chief contributors of colored effluents [1]. From environmental point of view, discharge of dyes into

the water resources even in a small quantity may cause skin irritation and allergic dermatitis. Few of them have been reported as mutagenic and carcinogenic for the aquatic organisms and humans [2–4]. Most of the dyes are stable to biodegradation as well as photodegradation [5–7]. Therefore, colored wastewater poses a challenge to the existing conventional wastewater treatment process. Thus far, many

*Corresponding author.

treatment methods such as membrane separation [8], electro-coagulation [9], coagulation and flocculation [10], oxidation or ozonation [11,12], and adsorption [13] have been used for removing dyes. Among these techniques, adsorption exhibited particular advantages over others because of its cheapness, simplicity of design, ease of operation, flexibility, effectiveness, and insensitivity to toxic pollutants and no harmful by-product to the treated water [14].

Superabsorbent hydrogels (SAHs) are a special class of solid adsorbents that are lightly physically or chemically cross-linked three-dimensional macromolecular polymeric networks, which have the ability to absorb huge amounts of aqueous fluids; and the absorbed fluids are hard to remove even under pressure. The selectivity, effectiveness, as well as reusability of these hydrogels adsorbents can be determined by the active chelating functional groups including carboxylic acid, sulfonic acid, amine hydroxyl, and amine group. These active functional groups adsorb, trap, and bind the adsorbate molecules and so make these SAHs as more effective adsorbent [15]. Several solid polymeric materials have been recently applied for the adsorption of dyes [16–24].

With the development and optimization of these different adsorbents, generation of the waste products also takes place in various industrial sectors. These waste products mainly consist the already used adsorbents that were used for the adsorption process. Therefore, after adsorption of adsorbate molecules, regeneration and reuse of the applied adsorbents is a problem. Conventionally, huge amount of solvent is used as eluent medium to wash and recover these adsorbents for recycle use. However, the produced waste eluent usually needs further treatment to avoid the secondary pollution. Usually, there are two general processes to treat these waste adsorbents. Firstly, these waste adsorbents may be recycled for further adsorption process via regenerating them in elution medium for again next cycle [25]; secondly, they can be disposed or cremated. When the adsorption process proceeded and reached to equilibrium condition, the original polymeric network backbone structure of adsorbent SAHs changed (due to an embedding layer of the present adsorbate molecules that are stable in their optimized conditions), and these network can function as a new kind of adsorbent. The alteration in original polymeric structure after adsorption can provide a new potential and effective way to utilize these already used SAHs adsorbents, which were after the adsorption process either discarded or may be regenerated in the acidic/alkaline medium.

Humic acid, a principal component of humic substances, consists of various multifunctional aliphatic

components as well as aromatic constituents with the large number of active functional hydrophilic groups (including carboxylates and phenolic hydroxyls groups, NH_2 groups and oxygen as well as nitrogen as bridge units) [26]. Because of the existence of these carboxylate and phenolate functional groups, sodium humate forms complexes/chelates with metal ions/dye molecules. Acrylic acid is smart in nature, cheap, highly hydrophilic and acts as an efficient chelating agent. Polyacrylamide is highly hydrophilic, has good biocompatibility as well as excellent resilience, permeability to oxygen and its functional pendant amide group works as effective chelating group for the different ionic and polar species.

The adsorption capacity of various adsorbents is highly influenced by various adsorption conditions. Yi et al. [27] synthesized SAHs based on sodium humate \poly (N-isopropylacrylamide) by solution polymerization and investigated its swelling and decoloring properties. Li Wang et al. [28] have carried out the removal of methylene blue (MB) dye from aqueous solution onto chitosan-g-poly (acrylic acid)/attapulgitite composites (CTS-g-PAA/APT) as adsorbent and studied the effects of concentration of attapulgitite (APT), temperature, and initial pH value of the dye solution on adsorption.

In our previous report, we have synthesized a biodegradable multifunctional SAHs based on acrylic acid and acrylamide monomers which is modified through sodium humate, and applied this as a solid adsorbent for removal of MB dye molecules [29]. The poly(AAc/AM/SH) SAHs were anionic in nature thus shows higher affinity towards cationic MB dye molecules, but it hardly adsorbs anionic dye molecules such as methyl orange (MO) due to its characteristics of negative charge existing on the polymeric surface. The adsorption of MB dye molecules makes it positively charged moiety and so it is being capable of MO molecules adsorption. Therefore, these MB molecules loaded SAHs without any prior treatment functions as a new kind of adsorbent.

The present investigation deals with an economical and efficient method to treat a waste adsorbent, thus introduces a new potential method to use an already used SAHs adsorbent without undergoing any regeneration or purification treatment. The experiments were performed to investigate the effects of different experimental parameters such as contact time, pH, temperature, dye concentration, and ionic strength on the adsorption to evaluate the optimum conditions for the MO dye molecules adsorption from aqueous solution. Adsorption models fit to equilibrium adsorption isotherm as well as kinetic data were also evaluated. Various thermodynamic parameters for the adsorption

phenomenon of MO dye molecules were also investigated. Desorption efficiency and reusability of the solid SAHs adsorbent were assessed on the basis of five consecutive adsorption—desorption cycles.

2. Experimental

2.1. Materials

Acrylic acid ((AAc), analytical grade), acrylamide ((AM), analytical grade), ammonium per sulfate ((APS), analytical grade), sodium hydroxide ((NaOH), analytical grade), *N,N*-methylene bisacrylamide ((NMBA), analytical grade), hydrochloric acid (HCl), and sodium chloride (NaCl) were purchased from CDH New Delhi, India. Methanol (analytical grade) was purchased from Qualikems, New Delhi, methylene blue and MO dye (spectroscopic grade) were purchased from Qualigens Fine Chemicals, Mumbai, India. Acrylamide was recrystallized from methanol before use. Sodium humate ((SH), analytical grade), (supplied from Aldrich) was used as received. Double distilled water was used throughout the experiments.

2.2. Synthesis of poly(AAc/AM/SH) SAHs

The detailed synthesis and the absorption behavior of poly(AAc/AM/SH) SAHs were reported in our previous study [29], in short the synthesis of poly(AAc/AM/SH) SAHs can be described as-AAc (7 g) and AM (7 g) both were dissolved in 30 ml distilled water. After dissolving, the reaction mixture was neutralized with NaOH solution, then the reaction solution was poured in a 250-ml three-neck round-bottom flask having a stirring rod, a nitrogen inlet as well as a reflux condenser. Then, cross-linker NMBA (0.20 wt.% of total monomer) was added to the monomer solution and subsequently dispersed SH (0.35 g) into the solution. The reaction mixture was stirred continuously for 30 min under nitrogen atmosphere to remove the dissolved oxygen. After this, the mixed reaction solution was heated for 1 h in a thermostat oil bath at 60°C. Then, the reaction initiator, APS (0.40 wt.% of total monomer), was introduced into the reaction flask. The solution was again stirred continuously for 2 h under nitrogen atmosphere at 60°C for homogeneity. After the reaction, the resulting reaction solution was poured in petri-dishes and then kept in a hot air oven for 2 h at 60°C to complete polymerization reaction and subsequent cross-linking process. On completion of reaction (after polymerization) in 2 h, the firm SAHs formed as thick sheet was then carefully removed. The produced SAHs sheet was cut into the small pieces (0.1–0.5 cm in thickness). Thereafter,

the unreacted monomers were separated by washing with methanol and then followed by swelling in water for 4 h. The washed SAHs were dried in an oven at 60°C to the constant weight. The dried SAHs were stored in desiccators.

2.3. Preparation of MB dye loaded poly(AAc/AM/SH) SAHs

To prepare the MB dye molecules loaded poly(AAc/AM/SH) SAHs, 50 mg of dry SAHs was introduced in 100 ml of MB dye molecules solution (initial ion concentration 320 mg/l) and left in solution for 48 h. The SAHs samples were taken out at different time intervals (1, 2, 3, 4, 5, 6, 7, 8, 9, 10, 11, 12, 24, and 48 h), then 2 ml of aqueous solution was sampled and analyzed for MB dye molecules content left in solution. The initial and final MB dye molecules content in the aqueous solution was analyzed with UV–vis spectroscopy. The adsorption capacity of the SAHs for MB dye molecules was calculated through the following expression:

$$q_e = \frac{C_o - C_e}{m} \times V \quad (1)$$

where q_e is the amount of MB dye molecules adsorbed at equilibrium (mg/g), C_o is the initial concentration of MB dye molecules (mg/l), C_e is the equilibrium concentration of MB dye molecules (mg/l); V is the volume of the MB dye molecules (l); and m is the mass of used SAHs sample (g).

2.4. Desorption study of MB dye from poly(AAc/AM/SH)-MB SAHs

To evaluate the stability of MB dye molecules into poly(AAc/AM/SH)-MB SAHs during MO adsorption process, 50 mg of poly(AAc/AM/SH)-MB SAHs was introduced into 12 conical flasks with 100 ml of distilled water. The pH of aqueous solution of each conical flask was at 1.0, 2.0, 3.0, 4.0, 5.0, 6.0, 7.0, 8.0, 9.0, 10.0, 11.0, and 12.0, respectively. Then, after being shaken at $30 \pm 0.5^\circ\text{C}$, 180 rpm in a shaker, the aqueous solutions were filtered and tested for the desorbed MB dye molecules. The final MB dye molecules concentration in the aqueous condition was determined by above given method. The MB dye molecules desorption percentage was calculated by the amount of MB dye molecules adsorbed onto the SAHs surface and final MB dye molecules concentration in the desorption medium.

Desorption percentage was evaluated with the following equation:

$$\text{Desorption percentage} = \frac{\text{Amount of MB dye desorbed to the elution medium}}{\text{Amount of MB dye adsorbed on the superabsorbent hydrogel}} \times 100 \quad (2)$$

2.5. Adsorption analysis of MO dye molecules

For the determination of MO dye adsorption experiments, 50 mg the adsorbent poly(AAc/AM/SH)-MB SAHs was loaded into a conical flask with 100 ml of MO dye molecules solution in various initial concentrations. Then, after that the sealed flasks were put in a shaker bath at various constant temperatures ($\pm 0.5^\circ\text{C}$) for 48 h, and shaken at the 180 rpm. After the adsorption, the SAHs samples were taken out at various time intervals (1, 2, 3, 4, 5, 6, 7, 8, 9, 10, 11, 12, 24, and 48 h), then 2 ml of aqueous solution was sampled and tested for MO dye molecules content left in solution. The capacity of MO dye molecules was also calculated by applying Eq. (1).

To determine the influence of temperature on the adsorption capacity, different isotherms were established at 30, 45, and 60°C .

In order to do kinetic study, adsorption experiments were conducted as follows: 50 mg of SAHs adsorbent was suspended in 100 ml solution containing 250 mg/l of MO dye. Then, all the sealed flasks were put in shaker bath at temperature $30 \pm 0.5^\circ\text{C}$, shaken at the 180 rpm at different time intervals. Then the flasks were withdrawn at different times for the evaluation of MO dye molecules concentrations. The rate of MO dye molecules adsorption was evaluated from the content of MO dye molecules adsorbed at different times.

To study the effect of pH on MO dye molecules adsorption, experiments were performed at the various initial pH ranging between 1.0 and 12.0. The pH of aqueous solution was adjusted with help of 0.1 M/l HCl or 0.1 M/l NaOH solutions. Initial MO dye molecules concentration of 250 mg/l and 50 mg of SAHs adsorbent was used. The aqueous solutions were shaken for 48 h at $30 \pm 0.5^\circ\text{C}$.

The effect of ionic strength on the MO dye removal was investigated in the aqueous solution containing 250 mg/l MO dye and various concentrations of NaCl (0.1, 0.01 and 0.001).

2.6. Fourier transforms infrared spectroscopy studies

The Fourier transforms infrared spectroscopy spectra of poly(AAc/AM/SH) SAHs and poly(AAc/

AM/SH)-MB SAHs were recorded with Perkin Elmer Spectrophotometer by using solid pellet potassium

bromide (KBr) after completely drying the sample at 60°C up to constant weight.

2.7. Desorption and regeneration

In order to check the potential of reusability of the applied adsorbent and for the recovery of MO dye molecules, consecutive adsorption–desorption cycles were repeated for the five times using the SAHs adsorbent prepared following the procedure discussed in adsorption experiments. The poly(AAc/AM/SH)-MB samples were first equilibrated with MO dye molecules in a solution having initial concentration of 250 mg/l, at temperature $30 \pm 0.5^\circ\text{C}$, and for 48 h.

Desorption of MO dye molecules from the poly(AAc/AM/SH)-MB SAHs (having 134.00 mg/g) was carried out using 50 mg adsorbent in 500 ml of 0.1 M NaOH solution (elution medium) for 48 h. After being shaken at temperature $30 \pm 0.5^\circ\text{C}$, and 180 rpm in a shaker, the SAHs were taken out and then dried at 60°C for 24 h. The regenerated SAHs were used for further adsorption. The final MO dye molecules concentration in the aqueous solution was determined by UV-vis spectroscopy. Desorption ratio was measured from the amount of MO dye molecules adsorbed on the polymer surface and final MO dye molecules concentration in the elution medium.

The desorption ratio was evaluated with the help of Eq. (2).

To determine the reusability of the poly(AAc/AM/SH)-MB SAHs, consecutive adsorption–desorption cycle was done for the five times of the same SAHs sample.

3. Results and discussion

3.1. Characterization of poly(AAc/AM/SH)-MB SAHs

The macroscopic image of dried poly(AAc/AM/SH) SAHs, and swollen poly(AAc/AM/SH)-MB SAHs is shown in Fig. 1(a) and (b), respectively. It can be observed that the surface appearance of dried poly(AAc/AM/SH) SAHs was rectangular in shape (0.1–0.5 cm in thickness), hard and dark browned

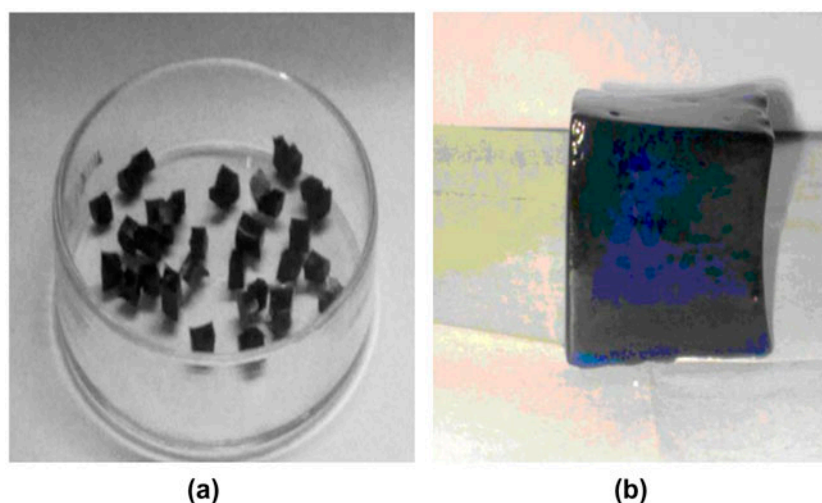


Fig. 1. (a) Macroscopic image of poly(AAc/AM/SH) SAHs and (b) macroscopic image of poly(AAc/AM/SH) SAHs on swelling in MB dye solution.

color. The swollen poly(AAc/AM/SH)-MB SAHs were soft, but it is strong enough to retain its shape and dark blue in color. This observation reveals that the MB dye molecules were adsorbed onto the surface of poly(AAc/AM/SH) SAHs.

The molecular structure of poly(AAc/AM/SH) SAHs consists free $-\text{COOH}$ and $-\text{OH}$ groups onto the backbone, MB dye molecules were attached with these active functional groups. The equilibrium removal capacity of poly(AAc/AM/SH) SAHs for MB dye molecules was 269 mg/g at 30°C .

The FTIR technique was used for the characterization of poly(AAc/AM/SH) SAHs before and after the adsorption of MB dye molecules. Fig. 2 displays the FTIR spectrum of (a) cross-linked poly(AAc/AM/SH) SAHs (b) poly(AAc/AM/SH)-MB SAHs. A broad band present at $3,447\text{ cm}^{-1}$ was assigned to $-\text{NH}$ stretching vibrations of the $-\text{NH}_2$ group (acrylamide),

and the overlapping absorption bands of $\text{O}-\text{H}$ group due to hydrogen bonding and acrylic acid were broadened after the adsorption and appeared at $3,436\text{ cm}^{-1}$ because of combined interaction of MB dye molecules with the $-\text{OH}$. The characteristic band at $1,715\text{ cm}^{-1}$ corresponding to $\text{C}=\text{O}$ group of carboxyl group after adsorption of MB dye molecules appeared at $1,690\text{ cm}^{-1}$. The presence of absorption band at $1,560\text{ cm}^{-1}$ attributed to symmetric stretching of the carboxylate group and at $1,400\text{ cm}^{-1}$ corresponding to asymmetric stretching of the carboxylate groups was shifted at $1,520$ and $1,452\text{ cm}^{-1}$, respectively. On the basis of FTIR analysis, it may also be concluded that the MB dye molecules adsorption onto the poly(AAc/AM/SH) SAHs surface mainly takes place through chelation and ion exchange mechanism between positively charged MB dye molecules and carboxylates as well as phenolic hydroxylics.

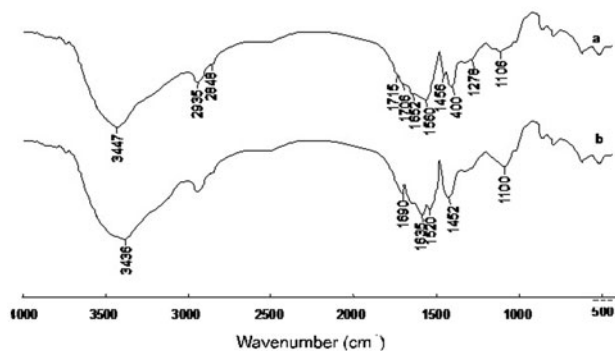


Fig. 2. FTIR spectrum of (a) crosslinked poly(AAc/AM/SH) SAHs and (b) poly(AAc/AM/SH)-MB SAHs.

3.2. Effect of pH on the desorption behavior of MB dye molecules from poly(AAc/AM/SH)-MB SAHs

In order to minimize the chance of leakage of MB dye molecules during the MO dye molecules adsorption, the stability of poly(AAc/AM/SH)-MB SAHs is one of important aspects for the application of poly(AAc/AM/SH)-MB SAHs as a MO dye adsorbent. So, for the practical application of poly(AAc/AM/SH)-MB SAHs as an adsorbent for MO dye molecules, it is necessary to study the stability of poly(AAc/AM/SH)-MB SAHs in various pH conditions firstly under the identical conditions as the adsorption process for MO dye containing water. The percent released of MB dye

molecules from poly(AAc/AM/SH)-MB SAHs at various pH range is shown in Fig. 3. It can be observed from the figure that concentration of remaining MB dye molecules is intensively dependent on the pH range of aqueous solution. At lower pH range (pH < 2.0) the desorption of MB dye molecules occurs extensively (>85%), because of competitive adsorption of protons for the active adsorption sites through substituting the MB dye molecules from the MB loaded SAHs surfaces (Fig. 4). Then, on further increasing the pH range (pH > 4.7) desorption of MB dye molecules decreased sharply and the SAHs shows very little desorption. This effect can be explained due to the formed chemical bonding because of chelation of the present $-\text{COOH}$, and $-\text{OH}$ functional groups with the MB dye molecules (Figs. 5 and 6). This made the high stability of poly(AAc/AM/SH)-MB SAHs. The

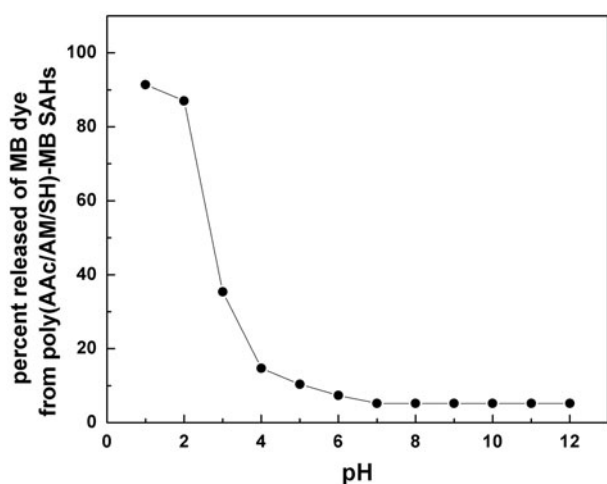


Fig. 3. Effect of pH on percent released of MB dye from poly(AAc/AM/SH)-MB SAHs, temperature $30 \pm 0.5^\circ\text{C}$.

given observation reveals that the poly(AAc/AM/SH)-MB SAHs were stable enough at the high pH range (pH > 5.0) and so can be effectively applied as an adsorbent for MB dye molecules.

3.3. Adsorption mechanism

Many investigations have been done on the binding of dyes to polyelectrolytes. Two possible mechanisms for MB adsorption can be considered. Firstly, interaction between the positively charged dye and negative active adsorption site of the adsorbent occurs mainly because of electrostatic forces as well as due to the formation of coordinate bonds [26]. These interactions occur at the adsorbate/adsorbent interface, and adsorption occurs with the groups phenolic hydroxyls and carboxylates as these groups have high affinities for cationic dyes [15,30], thus an ionic complex formed between the imines groups of MB dye and charged functional groups of SAHs. The other type of interactions may be hydrophobic and hydrogen bonding. Hydrophobic interaction is specifically aqueous solutions interaction that in the present case involves aromatic rings and the methane and methyl groups on the SAHs. Hydrogen bonding may exist between the reactive $-\text{OH}$ or $-\text{COOH}$ groups of SAHs chains and the amine groups of MB dye (Fig. 5(a)).

The findings of IR study (i.e. shift in characteristic asymmetric stretching of carboxylate and $\text{C}=\text{O}$ group of carboxyl group and) also confirmed the involvement of $-\text{COO}^-$ and $-\text{COOH}$ functional group in the adsorption mechanism.

Adsorption of MO dye occurs due to strong electrostatic interaction between MB enwrapped poly (AAc-AM-SH) and MO dyes. The possible adsorption mechanism is shown in Fig. 5(a) and (b).

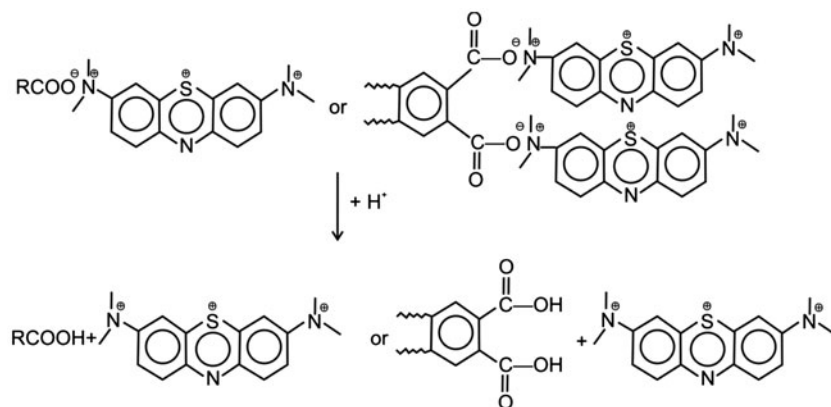


Fig. 4. Desorption of MB dye from poly(AAc/AM/SH)-MB at pH 3.0 via competitive adsorption of protons by substituting MB dye molecules.

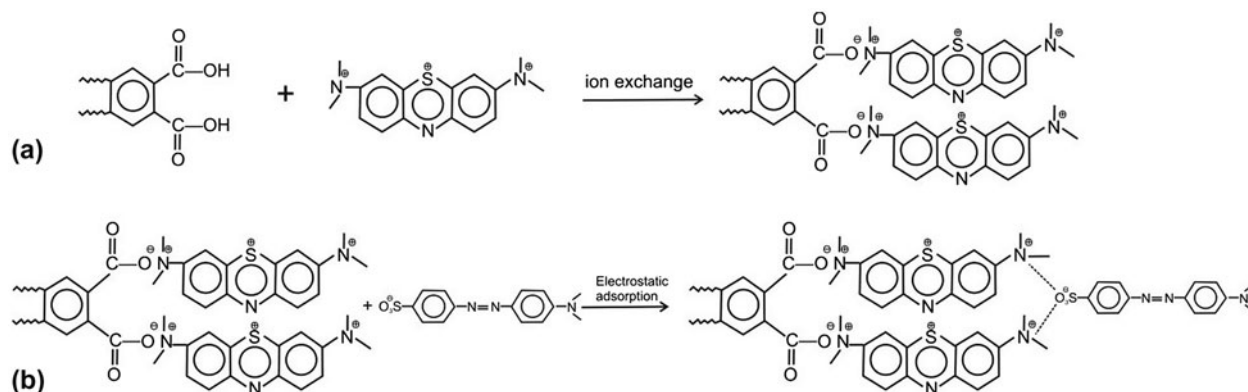


Fig. 5. Adsorption mechanisms of (a) MB adsorption onto poly (AAc/AM/SH) SAHs and (b) MO adsorption onto poly (AAc/AM/SH)-MB SAHs.

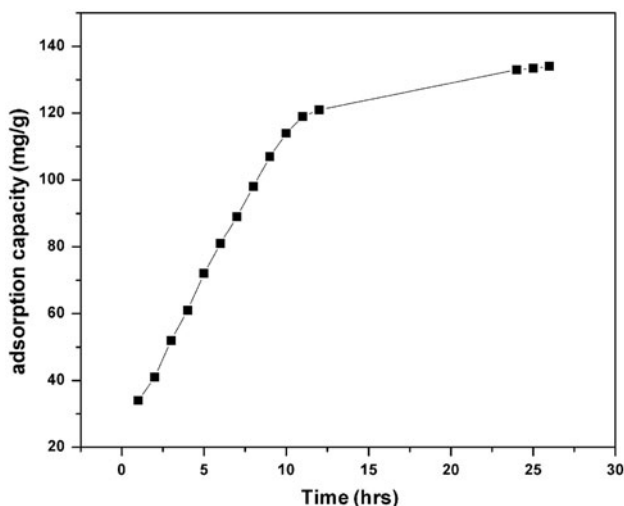


Fig. 6. Effect of contact time on the MO dye adsorption onto poly(AAc/AM/SH)-MB SAHs [initial ion concentration, 250 mg/l; temperature $30 \pm 0.5^\circ\text{C}$; hydrogel content, 50 mg].

3.4. Effect of contact time on adsorption of MO dye molecule

To observe the influence of contact time on the adsorption of MO dye molecules onto poly(AAc/AM/SH)-MB SAHs from aqueous solution, SAHs were equilibrated with the MO dye aqueous solution for predetermined time period. Fig. 6 displays the influence of contact time on the MO dye uptake. As observed from Fig. 6, the adsorption of MO dye molecules increases rapidly with the increase in contact time at initial state and then obtained a constant value beyond which no MO dye molecule was further adsorbed from its aqueous solutions. The MO adsorption curve was smooth as well as continuous leading

to saturation point. More than 88% of the equilibrium adsorption amount occurred within 10 h. This is explained as a fact that, initially the adsorption binding sites were vacant and MO molecules may easily interact with these void sites. The MO dye molecules removed almost remained constant after 27 h, and on further increasing of time, the adsorption efficiency hardly increased, so 27 h can be considered as the maximum equilibrium contact time. At the equilibrium state, the amount of MO dye desorbed from the SAHs was in dynamic equilibrium with the concentration of MO dye being adsorbed on the SAHs surface. The results suggest that the MO dye adsorption was fast in initial time, and thereafter, it becomes slower at near the equilibrium state. This can be explained because of the availability of more number of vacant active surface sites for the MO adsorption during initial stage, but as adsorption proceeded to equilibrium, the residual vacant adsorption sites were now became difficult to be occupied due to existing repulsive forces among the solute molecules present on the solid and bulk phases.

3.5. Effect of pH and ionic strength of dye solution on MO dye adsorption

The pH of aqueous solution is one of the most important factors, which might influence the adsorption capacity for dyes. It influences the solution chemistry of the different dyes (such as complexation and hydrolysis) as well as to the protonation of the various active functional groups present onto the adsorbents surface [31]. In the present investigation, influence of pHs on adsorption amount of MO dye molecules was examined at various initial pHs (1.00–12.0). Fig. 7 showed pH dependence of poly(AAc/AM/SH) SAHs

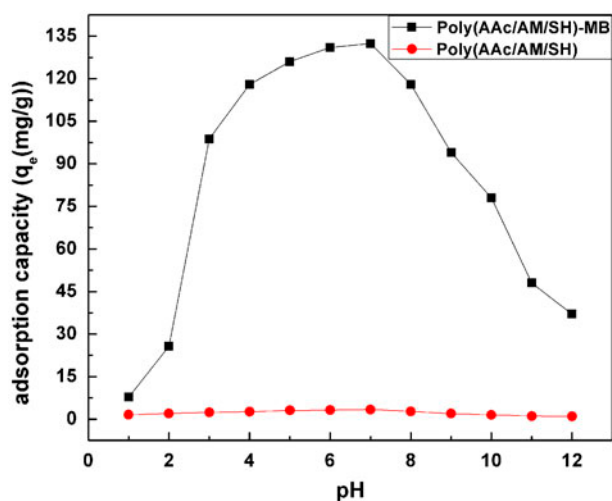


Fig. 7. Effect of pH on the adsorption of MO dye onto poly(AAc/AM/SH) SAHs and poly(AAc/AM/SH)-MB SAHs [contact time, 27 h; initial ion concentration, 250 mg/l; temperature $30 \pm 0.5^\circ\text{C}$; hydrogel content, 50 mg].

and poly(AAc/AM/SH)-MB SAHs for removal of MO dye from aqueous solution. It was observed from the Fig. 10 that poly(AAc/AM/SH)-MB SAHs show higher adsorption capacity than the poly(AAc/AM/SH) SAHs, which exhibit negligible adsorption in all measured pH ranges studied. This suggests that the incorporation of the MB dye onto the SAHs surface is favorable for enhancement of the adsorption capacity and thus played an important role in MO dye adsorption. Initially, the MO dye uptake increases sharply on increasing the initial pH (2–5) and then increased slowly until obtain a maximum adsorption of 134.00 mg/g at pHs 6.8. Afterthat with the increment

in pH, it goes down. It shows practically pH-independent behavior in pH range of 6.2–7.6. These findings can be interpreted as follows. At low pH, MB dye molecules desorbed from the poly(AAc/AM/SH)-MB SAHs, and for the poly(AAc/AM/SH) SAHs, on one hand, strong competition exists between hydrogen ions and MO dye molecules for the active binding sites, which made the availability of MO dye molecules to the active adsorption sites difficult to occur; on the other hand, after the leaking of MB dye molecules from the poly(AAc/AM/SH)-MB SAHs, the COO^- ions present onto the SAHs network were transformed into their protonated form and hinder the interaction of poly(AAc/AM/SH) SAHs with MO dye molecules, so the removal capacity for the MO dye molecules decreases (Fig. 4). Conversely, at the higher pH range ($4 < \text{pH} < 7.6$), amount of MB dye molecules attached on poly(AAc/AM/SH) SAHs was not released and as they are the active binding site for MO dye molecules. Therefore, increase in interaction between MO dye molecules and SAHs poly(AAc/AM/SH) SAHs that results in an increase in MO dye molecules adsorption (Fig. 8(a)). However, the adsorption amount was dramatically decreased on further increasing the pH range. This effect was because of the higher concentration of the hydroxide anions at a higher pH value, and having strong competition with MO dye molecules for the active adsorption binding sites of SAHs poly(AAc/AM/SH)-MB (Fig. 8(b)). Clearly, it can be seen that the pH of the aqueous solution plays very important role for the adsorption of MO dye molecules.

In case of typical dyeing system, it is well known that the presence of salts may either accelerate or retard the dye adsorption processes. Sodium chloride is frequently applied as a stimulator in various dyeing

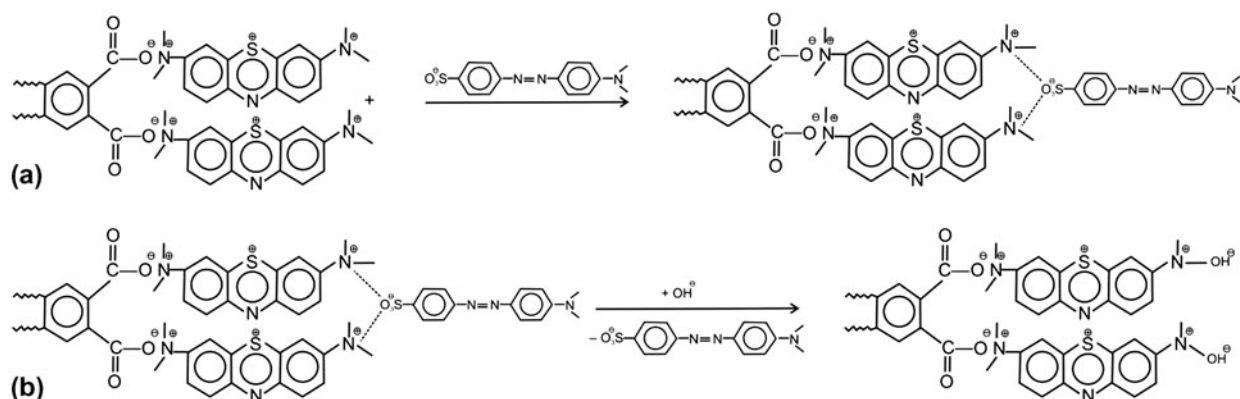


Fig. 8. (a) Model of adsorption of MO dye onto poly(AAc/AM/SH)-MB SAHs at pH ($2 < \text{pH} < 8$) and (b) Model of competitive adsorption of hydroxide ions onto poly(AAc/AM/SH)-MB SAHs at higher pH value (pH 8).

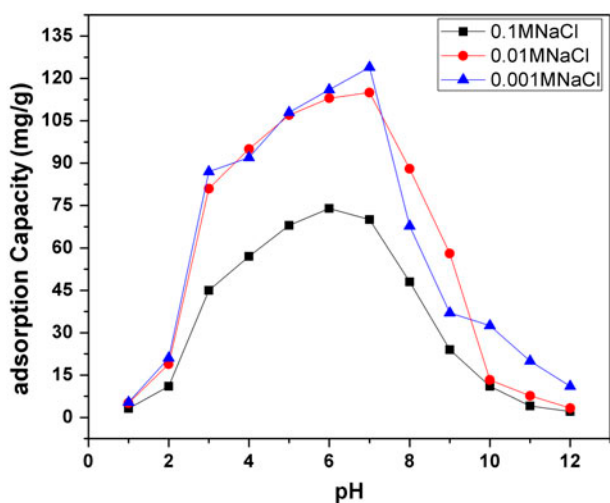


Fig. 9. Effect of ionic strength on the MO dye adsorption onto the poly(AAc/AM/SH)-MB SAHs [contact time, 27 h; initial ion concentration, 250 mg/l; temperature 300.5°C; hydrogel content, 50 mg].

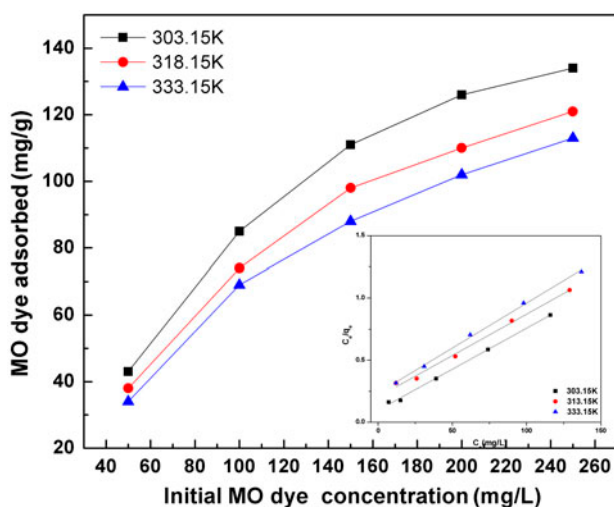


Fig. 10. Variation in the adsorption capacity as a function of initial MO dye concentration using poly(AAc/AM/SH)-MB SAHs. Inset figure: Langmuir adsorption isotherm of MO dye adsorption.

process. The influence of external ionic strength on the adsorption rate of MO dye on the poly(AAc/AM/SH)-MB SAHs was investigated in NaCl solutions with the concentration ranging from 0.001 to 0.01 M at 30°C. Fig. 9 shows the effect of ionic strength on the MO removal at various pH values. Generally, as the ion strength increased the adsorption capacity decreased, when the electrostatic attraction exists between the adsorbent surface and adsorbate mole-

cules. It can be observed from the Fig. 9 that at low sodium chloride content (0.001–0.01 M); the maximum adsorption capacity (124 and 115 mg/g) was obtained from pH 4 to 7, while in case of higher concentration (0.1 M), the maximum phosphate adsorption capacity (74 mg/g) was achieved from pH 2.5 to 6. The possible reason for low adsorption capacity at high ionic strength is due to the screening of electrostatic interaction of opposite charges by the salt on the adsorbent surface.

3.6. Effect of initial concentration of MO dye molecules on adsorption capacity of the poly(AAc/AM/SH)-MB SAHs

Initial ion concentration is one of the important parameter as initial concentration of MO dye molecules affects the adsorption amount of MO dye molecules and adsorption kinetics, so the influence of initial concentration on removal capacity was investigated. Fig. 10 displays the adsorption amount of MO dye molecules onto the poly(AAc/AM/SH)-MB SAHs as a function of varying initial MO dye concentrations ranging from 50 to 250 mg/l. It may be observed from the Fig. 10 that removal capacity of MO dye molecules increased (from 43 to 134 mg/g) with the increase in initial concentration of MO dye molecules solution if the content of adsorbent was constant. On reaching a maximum (134.00 mg/g) at 250 mg/l, it became nearly constant. This phenomenon can be explained as a fact of increase in driving force of the concentration gradient at the higher initial MO dye molecules concentration. It may also be observed that at the beginning, the adsorption is fast as well as increases gradually with progress of adsorption reaction or with the increase in initial concentration of MO dye molecules, amount of removed MO dye molecules increased but its adsorption percentage decreased. In case of lower initial concentration, the ratio of number of MO dye molecules to the available active binding sites is low; so, the fractional adsorption of MO dye molecules becomes independent of initial concentration. However, at the higher initial concentration, on the other hand, the number of available active adsorption become lesser, and therefore, subsequently, the adsorption of MO dye molecules depends on the initial concentration.

3.7. Adsorption isotherms

Adsorption characteristics and the equilibrium data, commonly known as adsorption isotherm, are fundamental in describing the interaction between adsorbate molecules and adsorbent, and so,

adsorption isotherms are critical in optimizing the application of adsorbent. The correlation of equilibrium experimental data applying either a theoretical or empirical equation is necessary for the adsorption interpretation as well as for prediction of the extent of adsorption. The adsorption experimental data are generally evaluated with the Langmuir, Freundlich, and Dubinin–Radushkevich (D–R) equilibrium adsorption isotherm models.

The Langmuir adsorption model is based on the assumption (1) maximum adsorption capacity corresponds to a saturated monolayer of adsorbate molecules on the adsorbent surface, (2) adsorption energy is equivalent, and (3) there is no transmigration of adsorbate molecules in the adsorbent surface. The adsorption data of MO dye molecules with the poly (AAc/AM/SH)-MB SAHs have been interpreted by applying this model. It is a mathematical model and displays a quantitative relationship between the concentration of MO dye molecules in the solution, and the amount of MO dye molecules adsorbed onto the adsorbent surfaces when two existing phases are at equilibrium. Langmuir adsorption isotherm equation may be represented as [32,33]

$$\frac{C_e}{q_e} = \frac{1}{K_e q_{\max}} + \frac{C_e}{q_{\max}} \quad (3)$$

where K_e (equilibrium sorption constant (l/mg)) and q_{\max} (maximum adsorption of MO dye molecules (mg/g)), C_e is equilibrium concentration of MO dye molecules in the solution (mg/l), q_e the amount of MO dye molecules adsorbed at equilibrium mg/g. The values of Langmuir constants and regression coefficients were evaluated through the linear plots of C_e/q_e versus C_e and shown in inset Fig. 10.

The Freundlich model is applied to describe reversible adsorption, and this is not restricted to the production of the monolayer. The Freundlich model provides an expression encompassing the heterogeneous surface system with the exponential distribution

of active adsorption sites and their energies. It also characterizes reversible adsorption. The Freundlich model may be described as follows [34];

$$\log(q_e) = 1/n \log(C_e) + \log K_f \quad (4)$$

where K_f (l/g) is Freundlich constant related with removal capacity and $1/n$ (dimensionless) parameter is related with intensity or energy of adsorption. The factors K_f and $1/n$ can be obtained through the intercept and slope of the linear plot of $\log q_e$ versus $\log C_e$, respectively.

The equilibrium adsorption data are also subjected to the D–R adsorption isotherm model to investigate the nature of adsorption as a physical or chemical adsorption process onto both homogeneous as well as heterogeneous surfaces [35]. The D–R adsorption isotherm equation can be presented by the following relationship:

$$\ln q_e = \ln q_m - \beta \varepsilon^2 \quad (5)$$

Here, constant β is correlated to mean free energy of adsorption process $((M/J)^2)$, q_m is the theoretical equilibrium adsorption capacity and ε is the Polanyi potential, it is related to the equilibrium MO dye molecules concentration (J/M), illustrated as follows:

$$\varepsilon = RT \ln(1 + 1/C_e) \quad (6)$$

Here, R ((8.314 J/(M K)) is gas constant and T (K) is absolute temperature. The D–R parameters may give valuable information regarding the mean free energy, E (J/mol), and it can be evaluated with the help of constant β , [36]: by using the following equation:

$$E = (2\beta)^{0.5} \quad (7)$$

The various constant parameters with the regression coefficients obtained from Langmuir, Freundlich, and

Table 1
Estimated various adsorption isotherm parameters for the MO dye adsorption onto poly (AAc/AM/SH)-MB SAHs from aqueous solutions

Temperature (K)	Langmuir model				Freundlich model			D–R equation			
	q_e (mg/g)	q_{\max} (mg/g)	$K_e \times 10^2$ (L/mg)	R^2	K_f (mg/g)	n	R^2	q_m (mg/g)	$\times 10^6$ (M ² /kJ)	R^2	E (kJ/M)
303.15	134	151.51	6.80	0.99	24.87	2.64	0.97	123.96	33.65	0.95	11.60
318.15	121	149.25	4.09	0.99	24.15	2.14	0.88	107.11	26.26	0.90	10.24
333.15	113	138.88	3.05	0.99	13.70	2.27	0.91	96.54	23.85	0.90	9.76

D–R adsorption isotherm equations mentioned above are tabulated in Table 1. The fit of the experimental data for MO dye molecules adsorption suggests that the regression coefficients values of Langmuir adsorption isotherm model were higher than of Freundlich as well as D–R adsorption models that show, the Langmuir adsorption isotherm model well fitted to the equilibrium data than the others two. The obtained q_{\max} values of the poly(AAc/AM/SH)-MB SAHs evaluated by Langmuir adsorption isotherm model were quite consistent with the experimental values (Table 1). The Langmuir isotherm model applicability indicates favorable monolayer adsorption with the involvement of chemical adsorption mechanism in MO dye molecules adsorption process. In addition to this the obtained q_{\max} value decreases on increasing the temperature and the similar type of behaviors are also observed by the removal capacities (K_f and q_{\max}) as well. The empirical parameter $1/n$ lying in the range $0 < 1/n < 1$ thus shows a favorable adsorption and the higher values of K_f signifies higher affinity of the poly(AAc/AM/SH)-MB SAHs for the MO dye molecules, and. K_e and K_f both factors decrease at high temperature, so suggesting that the removal efficiency diminished at higher temperature. The observed results thus specify the exothermic nature of existing adsorption process. Furthermore, according to the evaluated data from the D–R adsorption isotherm model, the mean free adsorption energy (E) was primarily deduced as shown in Table 1. The higher E value (>8.0 kJ/M), although the R^2 values was less than 0.9, so meaning that adsorption rates of MO dye molecules onto poly(AAc/AM/SH)-MB SAHs is probably controlled through the chemical process.

3.8. Effect of temperature on the adsorption

Temperature is an important parameter that has a noticeable influence on the adsorption capacity of poly(AAc/AM/SH)-MB SAHs. Fig. 11 shows the representative graph for adsorption capacity of MO dye onto poly(AAc/AM/SH)-MB SAHs surface against different temperatures ranging from 20 to 60°C. It can be observed that with the increase in temperature from 20 to 30°C, the adsorption capacity increased from 117 to 134 mg/g. However, with further increase in temperature, it was observed that MO content decreased from 134 to 113 mg/g, with the increase in temperature from 30 to 60°C. The decrement in the adsorption capacity for MO dye molecules on increase in temperature revealed that the MO dye molecules adsorption was favorable at low temperature. As the adsorption process is an exothermic reaction, so it was expected that temperature increase in adsorption system would

result in decrease in adsorption capacity. Since, adsorption is a dynamic process and involves both adsorptions as well as desorption phenomenon. The adsorbate molecules (MO) are attracted through the surface force and so attach on the surface of the adsorbent. These adsorbate molecules are in constant motion also. The temperature increase causes an increase in the energy level of the adsorbed molecules. The high amount of energy speeds up the Brownian motion, and thus requiring stronger force for keeping the adsorbed molecules adhered onto the surface of adsorbent (high adsorption temperature, higher the velocity of the adsorbate molecules' Brownian motion, so resulting in reduction in the adsorption possibility of the adsorbate molecules MO). At the high temperature, the adsorbate has enough energy to resist the attraction force and thus migrate back from the solid phase to bulk phase. On the other hand, another reason is the existence of fewer number of active adsorption sites at the higher temperature that is due to the deactivation of the solid adsorbent surface or because of destruction of few active adsorption sites present on the adsorbent surface resulting from bond rupture. So, 30°C was selected as the adsorption temperature.

3.9. Thermodynamic parameters of adsorption

Temperature dependence for any adsorption phenomenon is accompanied with change in various

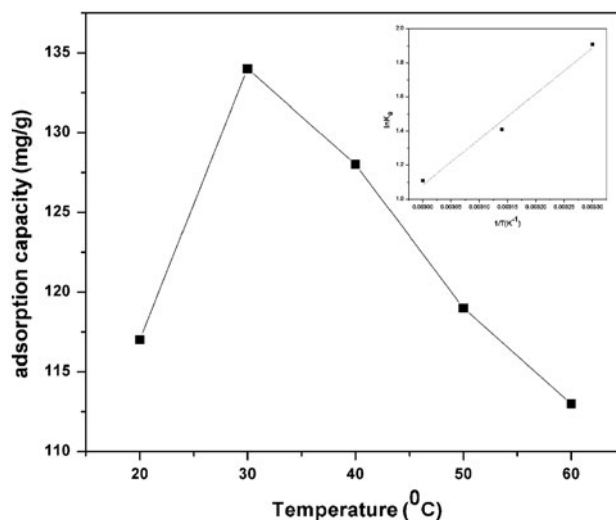


Fig. 11. Effect of temperature on the MO dye adsorption onto the poly(AAc/AM/SH)-MB SAHs [contact time, 27 h; initial ion concentration, 250 mg/l; hydrogel content, 50 mg]. Inset figure: Plot of $\ln K_e$ versus T^{-1} for the evaluation of thermodynamic parameters of the MO dye adsorption process.

thermodynamic parameters that includes Gibbs free energy change (ΔG), enthalpy change (ΔH), and entropy change (ΔS). These parameters are the real indicators for the practical utilization of an adsorption phenomenon. With these thermodynamic parameters, spontaneity of any adsorption process may be evaluated. The change in Gibbs free energy (ΔG) for an adsorption reaction was obtained by using following expression [37]:

$$\Delta G = \Delta G^0 + RT \ln K_e \quad (8)$$

At the point of equilibrium adsorption state, ΔG becomes zero, and so

$$\Delta G^0 = -RT \ln K_e \quad (9)$$

Here R , the universal gas constant ($8.314 \text{ J M}^{-1} \text{ K}^{-1}$), K_e , the Langmuir adsorption equilibrium constant and T , absolute temperature in Kelvin.

The standard entropy change and standard enthalpy change both at constant temperature are given by the relation;

$$\Delta G^0 = \Delta H^0 - T\Delta S \quad (10)$$

On adding the Eqs. (9) and (10), we get following expression:

$$\ln K_e = -\Delta G^0/(RT) = (\Delta S^0/R) - (\Delta H^0/(RT)) \quad (11)$$

Following the assumption that standard enthalpy change ΔH^0 for any reaction is approximately independent of temperature, so ΔH^0 can be evaluated from the slope of the linear plot of $\ln K_e$ versus $1/T$ with the equation

$$\Delta H^0 = [R(d \ln K_e / (d1/T))] \quad (12)$$

Table 2
Thermodynamic parameters for MO dye adsorption onto poly(AAc/AM/SH)-MB SAHs at various temperatures

Temperature (K)	MO dye			
	$\ln K_e$	ΔG^0 (kJ/M)	ΔH^0 (kJ/M)	ΔS^0 (J/MK)
303.15	1.91	-4.814		12.78
318.15	1.41	-3.068	-1.128	6.09
333.15	1.11	-3.074		5.84

Inset Fig. 11 represents the linear plots of $\ln K_e$ versus $1/T$. Changes in ΔS^0 and ΔG^0 may be considered to find whether the process is spontaneous or not. The change in Gibbs free energy change explains the spontaneous nature of the adsorption, and its higher negative value shows energetically favorable adsorption [16]. The obtained results of experiments are presented in Table 2. The determined Langmuir equilibrium constants at 303.15, 318.15, and 333.15 K were used to measure the thermodynamic parameters of adsorption process. Negative change in ΔG^0 suggests the feasibility as well as spontaneity of adsorption process; further with the increase in temperature, the decrement in the values of ΔG^0 reveals that the adsorption process was more spontaneous at the higher temperatures. The negative values of standard enthalpy change show that the MO dye molecules adsorption are exothermic, which is also supported by the decrease in adsorption capacity of MO dye molecules with rise in the temperature. The positive entropy change indicates the increase in randomness at the solid–solution interface during the MO dye molecules adsorption with few structural changes in MO dye molecules and adsorbent surfaces. Positive ΔS^0 also assigned to an increase in the degree of freedom for the adsorbate species [38].

3.10. Adsorption kinetics

Adsorption kinetics was calculated to establish the time course of MO dye molecules uptake on the poly(AAc/AM/SH)-MB SAHs. Examining whether the adsorption behavior of MO dye molecules may be described by a predictive theoretical model was also desirable. Adsorption kinetics may also be useful to understand adsorption process mechanism and to estimate the application performance of the adsorbents applied for the adsorbate adsorbed. Thus, the pseudo-first-order kinetic and the pseudo-second order kinetic both models were applied to analyze the experimental data obtained.

Lagergren pseudo-first order [39] and Ho and McKay's pseudo-second-order kinetics model [40] are two generally applied kinetic models applied for solid–liquid adsorption.

The Lagergren pseudo-first order is expressed as

$$\log(q_e - q_t) = \log q_e - k_1 t / 2.303 \quad (13)$$

where q_e (mg/g), and q_t (mg/g) are the amount of MO dye molecules adsorbed (mg/g) at equilibrium condition and at any time t , respectively. k_1 (min^{-1}) is rate constant of the pseudo-first-order model. k_1 and q_e

Table 3

Estimated various adsorption kinetic parameters for the MO dye adsorption onto poly(AAc/AM/SH)-MB SAHs in aqueous solutions

Temperature (K)	Pseudo-first-order model				Pseudo-second-order model			
	$q_{e, \text{exp}}$ (mg/g)	$q_{e, \text{cal}}$ (mg/g)	$k_1 \times 10^2$ (1/min)	R^2	$q_{e, \text{exp}}$ (mg/g)	$q_{e, \text{cal}}$ (mg/g)	$k_2 \times 10^3$ (g/mg min)	R^2
303.15	134.00	177.82	21.60	0.991	134.00	163.93	1.11	0.987
318.15	121.00	184.07	27.34	0.984	121.00	151.51	1.26	0.985
333.15	113.00	141.12	21.04	0.972	113.00	142.85	1.10	0.988

values may be calculated through the slope and intercept of the linear plot of $\log(q_e - q_t)$ versus t , and were presented in Table 3.

This adsorption kinetic model has been applied extensively to have account of the adsorption of metal ions/dyes on the adsorbents; however, pseudo first-order-kinetic model equation not fit well over the whole range of the contact time and chiefly applicable only over the initial phase of the adsorption process. The main drawbacks of pseudo first-order kinetic model are (1) the drawn plots are only linear for the first 11 h, approximately. After this initial 6-h time period the theoretical and experimental data, they do not correlate well, and (2) equilibrium adsorption amount determined with the linear equation was in poor agreement with the experimental q_e values.

It may be observed that there are much differences between the q_e values calculated and q_e values experimental ($q_{e, \text{exp}}$). In addition, the linear regression coefficients (R^2) of the pseudo-first-order kinetic model obtained among 0.972–0.991, and thus suggesting that MO adsorption process does not fit good to pseudo-first-order kinetic model.

Pseudo-second-order kinetic models were expressed by the following equation

$$t/q_t = 1/(k_2 q_e^2) + t/q_e \quad (14)$$

Here k_2 (g/(mg min)), rate constant of the pseudo-second-order kinetic model. The kinetics parameters q_e and k_2 were evaluated from slope and intercept of the linear plot of t/q_t against t (as shown in Fig. 12) and given in Table 3.

It can be seen from Table 3 that the obtained q_e values of the pseudo-second-order kinetic model were in good agreement with the experimental $q_{e, \text{exp}}$ values. Moreover, the values of linear regression coefficients (R^2) of the pseudo-second-order kinetic model found are over 0.985, which signifies that the pseudo-second-order kinetic model may be used for the whole MO adsorption process. The obtained results suggested

that the investigated adsorption process related to pseudo-second-order kinetic adsorption model, which reveals that the adsorption behavior of the poly(AAc/AM/SH)-MB was chemical adsorption.

3.11. Desorption/regeneration of adsorbent

For the practical application of the adsorbent, the adsorption as well as desorption processes was repeated five times to examine the potential application of the poly(AAc/AM/SH)-MB SAHs for recycling. As for its potential application, a good solid adsorbent in addition to its high adsorption efficiency should also exhibit a good regeneration capability. Wastewater treatment will be economical if the applied adsorbent can be recovered easily and repeatedly used. The poly(AAc/AM/SH)-MB SAHs that were used for MO dye adsorption were placed in 500 ml of 0.1 M NaOH solution for 48 h, and the amount of MO dye molecules desorbed to the elution medium was measured. Fig. 13 shows the desorption

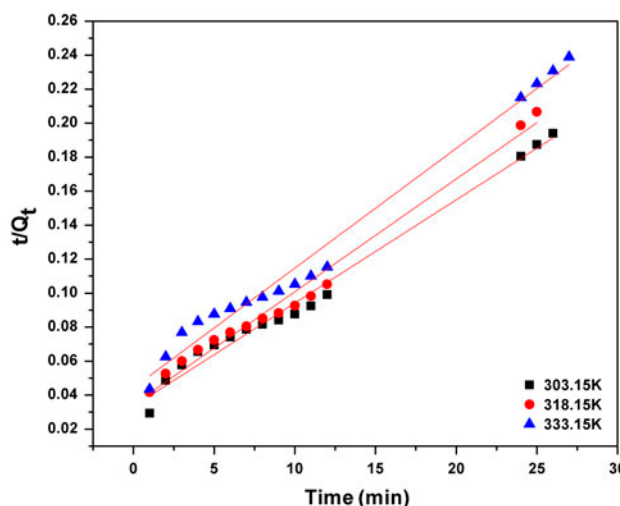


Fig. 12. Pseudo second order kinetics of MO dye adsorption onto poly(AAc/AM/SH)-MB SAHs.

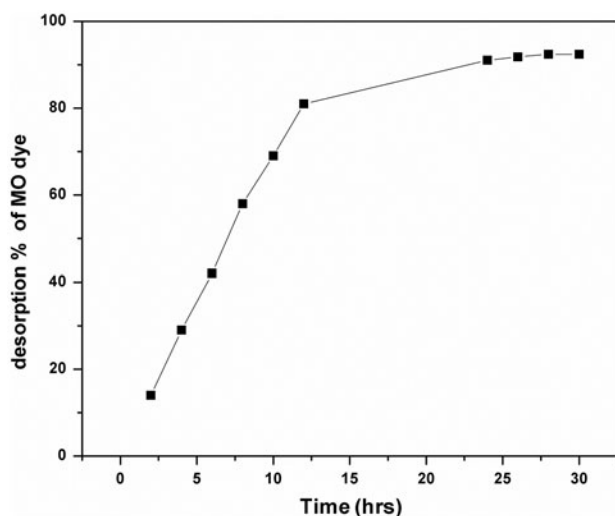


Fig. 13. Plot of desorption ratio for MO dye from poly (AAc/AM/SH)-MB SAHs as a function of time.

Table 4

Adsorption amount of MO dye after repeated adsorption-desorption cycle

Cycle no.	Adsorption capacity (mg/g)	Desorption (%)
1	134.00	92.42
2	132.05	92.00
3	130.98	91.08
4	130.00	90.00
5	129.45	88.66

ratio of poly(AAc/AM/SH)-MB SAHs (having 134 mg/g MO dye) as a function of time. The maximum desorption ratio observed was approximately 90% in 27 h. Table 4 displayed the experimental data for the adsorption capacity and the times for reuse for SAHs sample. Desorption capacity was generally high, and the adsorption efficiency was almost unaffected. After fifth cycles of adsorption—desorption operations, the MO adsorption capacity was around 129.45 mg/g. MO dye was desorbed in distilled water, as no MB dye molecules were desorbed to the elution medium at pH higher than eight. Thus, it can be concluded that, poly(AAc/AM/SH)-MB SAHs showed stable MO dye adsorption after repeated regeneration and so qualified for multiple practical application.

4. Conclusion

In this report, a new cost-efficient and cost-effective method for the treatment of a waste adsorbent poly(AAc/AM/SH)-MB SAHs was provided. The

already used adsorbents can be applied as new ones for different dye adsorption due to an altered surface structure. Poly(AAc/AM/SH) SAHs after the removal of MB dye can be used for the MO dye adsorption directly from its aqueous solution. Poly(AAc/AM/SH)-MB SAHs were proven to be stable enough and thus suitable to adsorb MO dye at a pH > 4.7. Maximum adsorption capacity of MO dye (134 mg/g) was achieved at pH 6.8. Increase in temperature results in decrease in adsorption capacity. Adsorption equilibrium isotherm and kinetics study reveals that the adsorption behavior was chemical monolayer adsorption for MO dye facile to bind with MB dye molecules. The thermodynamic analysis indicates that the adsorption process was exothermic as well as spontaneous in nature. The results of five-time consecutive adsorption–desorption cycle suggest that the MO dye can be desorbed easily and effectively, and the regenerated SAHs adsorbent can be reused again almost without any loss of adsorption efficiency for a few cycles, which seems the most efficient method to treat an already used adsorbent poly(AAc/AM/SH)-MB SAHs. The results also confirmed that poly (AAc/AM/SH)-MB SAHs can be used as effective solid adsorbent for the MO dye adsorption from waste water and aqueous effluents.

Supplementary material

The supplementary material for this paper is available online at <http://dx.doi.org/10.1080/19443994.2013.859098>.

Acknowledgment

This work was financially supported by the University Grant Commission New Delhi, India (39 875 2010).

References

- [1] K. Ravikumar, B. Deebika, K. Balu, Decolourization of aqueous dye solutions by a novel adsorbent: Application of statistical designs and surface plots for the optimization and regression analysis, *J. Hazard. Mater.* 122 (2005) 75–83.
- [2] P. Dutta, An overview of textile pollution and its remedy, *Indian J. Environ. Prot.* 14 (1994) 443–446.
- [3] K. Chen, J. Wu, C. Huang, Y. Liang, S.C. Hwang, Decolorization of azo dye using PVA-immobilized microorganisms, *J. Biotechnol.* 101 (2003) 241–252.
- [4] Y. Gong, M. Li Ding, C. Yang, H. Liu, Y. Sun, Utilization of powdered peanut hull as biosorbent for removal of anionic dyes from aqueous solution, *Dyes Pigm.* 8(64) (2005) 187–192.

- [5] W.T. Tsai, C.Y. Chang, M.C. Lin, S.F. Chien, H.F. Sun, M.F. Hsieh, Adsorption of acid dye onto activated carbons prepared from agricultural waste bagasse by $ZnCl_2$ activation, *Chemosphere* 45 (2001) 51–58.
- [6] J. Yener, T. Kopac, G. Dogu, T. Dogu, Adsorption of Basic Yellow 28 from aqueous solutions with clinoptilolite and amberlite, *J. Colloid Interface Sci.* 294 (2006) 255–264.
- [7] S. Wang, Y. Boyjoo, A. Choueib, A comparative study of dye removal using fly ash treated by different methods, *Chemosphere* 60 (2005) 1401–1407.
- [8] G. Ciardelli, L. Corsi, M. Marucci, Membrane separation for wastewater reuse in the textile industry, *Resour. Conserv. Recycl.* 31 (2000) 189–197.
- [9] A. Alinsafi, M. Khemis, M.N. Pons, J.P. Leclerc, A. Yaacoubi, A. Benhammou, A. Nejmeddine, Electrocoagulation of reactive textile dyes and textile wastewater, *Chem. Eng. Process.* 44 (2005) 461–470.
- [10] J. Panswed, S. Wongchaisuwan, Mechanism of dye wastewater color removal by magnesium carbonate-hydrated basic, *Water Sci. Technol.* 18 (1986) 139–144.
- [11] K. Swaminathan, S. Sandhya, A. Carmalin Sophia, K. Pachhade, Y.V. Subrahmanyam, Decolorization and degradation of H-acid and other dyes using ferrous–Hydrogen peroxide system, *Chemosphere* 50 (2003) 619–625.
- [12] M. Muthukumar, N. Selvakumar, Studies on the effect of inorganic salts on decolouration of acid dye effluents by ozonation, *Dyes Pigm.* 62 (2004) 221–228.
- [13] I.D. Mall, V.C. Srivastava, N.K. Agarwal, I.M. Mishra, Removal of congo red from aqueous solution by bagasse fly ash and activated carbon: Kinetic study and equilibrium isotherm analyses, *Chemosphere* 61 (2005) 492–501.
- [14] M. Mitchell, W.R. Ernst, G.R. Lightsey, Adsorption of textile dyes by activated carbon produced from agricultural, municipal and industrial-wastes, *Environ. Contam. Toxicol.* 19 (1978) 307–311.
- [15] E. Karadag, D. Saraydin, O. Guven, Behaviors of acrylamide itaconic acid hydrogels in uptake of uranyl ions from aqueous solutions, *Sep. Sci. Technol.* 30 (1995) 3287–3298.
- [16] K.S. Walton, J. Cavalcante, M.D. LeVan, Adsorption of light alkanes on coconut nanoporous activated carbon, *Braz. J. Chem. Eng.* 23 (2006) 555–561.
- [17] S.T. Ong, C.K. Lee, Z. Zainal, Removal of basic and reactive dyes using ethylenediamine modified rice hull, *Bioresour. Technol.* 98 (2007) 2792–2799.
- [18] M.S. Berber, R.L. Mendoza, P.A. Ramos, J. Davila, P.E. Mendoza, J. Flores, Comparison of isotherms for the ion exchange of Pb(II) from aqueous solution onto homoionic clinoptilolite, *J. Colloid Interface Sci.* 301 (2006) 40.
- [19] R. Jain, M. Mathur, S. Sikarwar, A. Mittal, Removal of the hazardous dye rhodamine B through photocatalytic and adsorption treatments, *J. Environ. Manage.* 85 (2007) 956–964.
- [20] B.S. Inbaraj, J.T. Chien, J. Yang, B.H. Chen, Effect of pH on binding of mutagenic heterocyclic amines by the natural biopolymer poly (γ -glutamic acid), *Biochem. Eng. J.* 31 (2006) 204–215.
- [21] S. Wang, H. Li, L. Xu, Application of zeolite MCM-22 for basic dye removal from wastewater, *J. Colloid Interface Sci.* 295 (2006) 71–78.
- [22] G. Crini, H.N. Peindy, F. Gimbert, C. Robert, Removal of C.I. Basic Green 4 (Malachite Green) from aqueous solution by adsorption using cyclodextrin-based adsorbent: Kinetic and equilibrium studies, *Sep. Purif. Technol.* 53 (2007) 97–110.
- [23] O. Hamdaoui, Batch study of liquid-phase adsorption of methylene blue using cedar sawdust and crushed brick, *J. Hazard. Mater.* 135 (2006) 264–273.
- [24] R. Dhodapkar, N.N. Rao, S.P. Pande, S.N. Kaul, Removal of basic dyes from aqueous medium using a novel polymer-Jalshakti, *Bioresour. Technol.* 97 (2006) 877–885.
- [25] A. Kara, L. Uzun, N. Besirli, A. Denizli, Poly(ethylene glycol dimethacrylate-*n*-vinyl imidazole) beads for heavy metal removal, *J. Hazard. Mater.* B106 (2004) 93–99.
- [26] W. Wang, A. Wang, Synthesis, Swelling Behaviors, and Slow-Release Characteristics of a Guar Gum-g-Poly(sodium acrylate)/Sodium Humate Superabsorbent, *J. Appl. Polym. Sci.* 112 (2009) 2102–2111.
- [27] J.Z. Yi, Y.Q. Ma, L.M. Zhang, Synthesis and decoloring properties of sodium humate/poly (N-isopropylacrylamide) hydrogels, *Bioresour. Technol.* 11 (2008) 5362–5367.
- [28] W. Li, J. Zhang, A. Wang, Fast removal of Methylene Blue from aqueous solution by adsorption onto chitosan-g-poly (acrylic acid)/attapulgit composite, *Desalination* 266 (2011) 33–39.
- [29] T. Singh, R. Singhal, Poly (acrylic acid/acrylamide/sodium humate) superabsorbent hydrogels for metal ion/dye adsorption: Effect of sodium humate concentration, *J. Appl. Polym. Sci.* 125 (2012) 1267.
- [30] E. Karadag, D. Saraydin, O. Guven, Use of superswelling acrylamide/maleic acid hydrogels for monovalent cationic dye adsorption, *Sep. Sci. Technol.* 30 (1995) 3747–3760.
- [31] W. Chouyyok, R.J. Wiacek, K. Pattamakomsan, T. Sangvanich, R.M. Grudzien, G.E. Fryxell, W. Yantasee, Phosphate removal by anion binding on functionalized nanoporous sorbents, *Environ. Sci. Technol.* 44 (2010) 3073–3078.
- [32] I.J. Langmuir, The adsorption of gases on plane surfaces of glass, mica and platinum, *J. Am. Chem. Soc.* 40 (1918) 1361–1403.
- [33] Y.S. Ho, C.T. Huang, H.W. Huang, Equilibrium sorption isotherm for metal ions on tree fern, *Process Biochem.* 37 (2002) 1421–1430.
- [34] M. Jaroniec, Physical adsorption on heterogeneous solids, *Adv. Colloid Interface Sci.* 18 (1983) 149–225.
- [35] T. Shahwan, H.N. Erten, Temperature effects in barium sorption on natural kaolinite and chlorite-illite clays, *J. Radioanal. Nucl. Chem.* 260 (2004) 43–48.
- [36] J.P. Hobson, Physical adsorption isotherms extending from ultrahigh vacuum to vapor pressure, *J. Phys. Chem.* 73 (1969) 2720–2727.
- [37] Y. Liu, Some consideration on the Langmuir isotherm equation, *Colloids Surf., A* 274 (2006) 34–36.
- [38] C. Raymon, *Chemistry: Thermodynamic*. McGraw-Hill, Boston, MA, 1998, p. 737.
- [39] S. Lagergren, K.S. Vetenskapsakademiens, About the theory of so called adsorption of soluble substances, *Handlingar* 24 (1898) 1–39.
- [40] Y.S. Ho, G. McKay, Pseudo-second order model for adsorption processes, *Process Biochem.* 34 (1999) 451–465.